

Supplementary Information

Hydrogen-Bonding-Catalyzed the Degradation of Polyethylene Glycol to 1,4-Dioxane over OH-functionalized Ionic Liquid

Huan Wang,^a Xue Zheng,^a Wei-Tao Wang,^a Zhen-Hong He,^a Kuan Wang,^a Weiping Wang,^a Jianchuan Liu,^{*d} Zhi-Hao Zhao,^{*c} and Zhao-Tie Liu^{*a, b}

^a Key Laboratory of Chemical Additives for China National Light Industry, College of Chemistry and Chemical Engineering, Shaanxi University of Science and Technology, Xi'an, 710021, China.

^b School of Chemistry & Chemical Engineering, Shaanxi Normal University, Xi'an, 710119, China. E-mail: ztliu@snnu.edu.cn

^c State Key Laboratory of Solidification Processing and School of Materials Science and Engineering, Northwestern Polytechnical University, Xi'an, Shaanxi, 710072, P. R. China. E-mail: zhaozhihao@nwpu.edu.cn

^d School of Electrical Engineering and Electronic Information, Xihua University, Chengdu 610039, China. liujianchuan@xhu.edu.cn

1. Experimental Procedures

1.1 Materials

Polyethylene glycol (PEG, average Mn: 200, 400, 600, 800 and 1000) was obtained from Tianjin Damao Chemical Reagent Co., Ltd. 1,4-Dioxane (99.7% with molecular sieves, stabilized with BHT), n-dodecane (>99.0%), tetraethylene glycol (99%), methyl sulfoxide-d₆ (DMSO-d₆, 99.8 atom% of D) and chloroform-d (CDCl₃, 99.8 atom% of D) were purchased from Macklin's Reagent Co., Ltd. Diethyl ether (>99.5%) was obtained from Sinopharm Chemical Reagent Co., Ltd. All chemical reagents were used as received.

Ionic liquids were obtained from the Center for Green Chemistry and Catalysis, Lanzhou Institute of Chemical Physics, Chinese Academy of Sciences, and freeze-dried before use, their chemical structures are provided in Fig. S1.

1.2 Instrumentation

NMR spectra were recorded on Bruker Avance III 400 HD or 500 WB spectrometer equipped with 5 mm pulsed-field-gradient (PFG) probes. Chemical shifts are given in ppm relative to tetramethylsilane (TMS). To eliminate the effect of solvent, wilmad coaxial insert NMR tubes were used for ¹H NMR, ¹⁹F NMR and ¹⁷O NMR at 333.15 K. DMSO-d₆ was added in the inner tube, and the sample was added in the outer tube. The product was quantitatively analyzed by using gas chromatography GC (GC9720, Fuli instrument) with a FID detector and a nonpolar capillary column (DB-5, 30 m × 0.25 mm × 0.25 μm). The GC-MS analysis was performed using gas chromatography-mass spectrometry (GC-MS, SHIMADZU-QP2010) with a packed column DB-5 MS.

All density functional theory (DFT) calculations were performed with the Gaussian 09 package.¹ Geometry optimizations were carried out at the M062X-D3²/def2-TZVP³ level at 393.15 K. The frequency calculations were carried out at the M062X-D3/def2-TZVP level using the optimized structures to confirm that the reactant and product have no imaginary frequencies and that the transition states (TSs) have only one imaginary frequency. The intrinsic reaction coordinate calculations were used to verify these TSs. Solvation corrections^{4, 5} were calculated by a self-consistent reaction field using the SMD-GIL model.

1.3 Detailed experimental procedure for polyethylene glycol degradation

All reactions were performed in a sealed tube (15 mL of inner volume) equipped with a magnetic stirrer. Typically, 40 mg of PEG (average Mn: 400) and 0.4 mmol of [HO-EtMIm][OTf] were sequentially added into the reactor and sealed under nitrogen atmosphere. Then the reactor was moved to an oil bath with the desired temperature (e.g., 130 °C) for 12 h. After reaction, the reactor was cooled down in ice water. For GC analysis, 2 ml of diethyl ether and 0.017 g of n-dodecane (the internal standard) were added to the reaction mixture. After vigorous stirring and centrifugation, the upper layer liquid (product phase) and the IL phase were collected, respectively. The products were qualitatively and quantitatively analyzed by GC-MS and GC, respectively. The standard curve of the product is shown in Fig. S3. And the yield of product was calculated according to the following equation:

$$\text{Yield of product} = \text{Moles of the product obtained} / \text{Theoretic moles of the product} \times 100\%$$

1.4 Recycling tests

The reusability of [HO-EtMIm][OTf] was tested as follows:

After reaction, the reaction mixture was centrifuged and the IL phase was collected through simple phase separation. Subsequently, the collected [HO-EtMIm][OTf] was distilled under vacuum to remove the generated H₂O. Then, the [HO-EtMIm][OTf] was directly reused for the next run.

2. Additional data

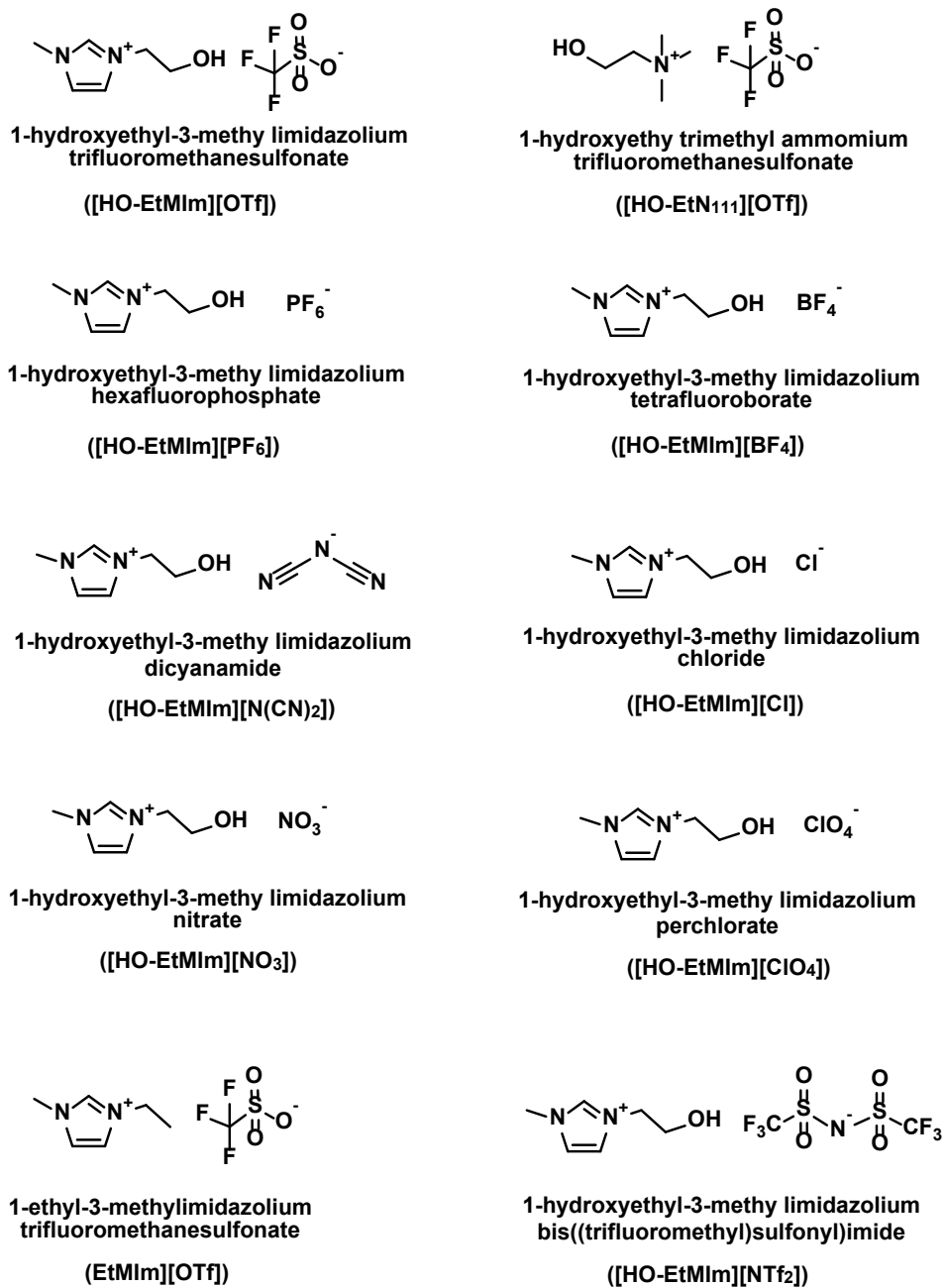


Fig. S1 The ILs used in this work.

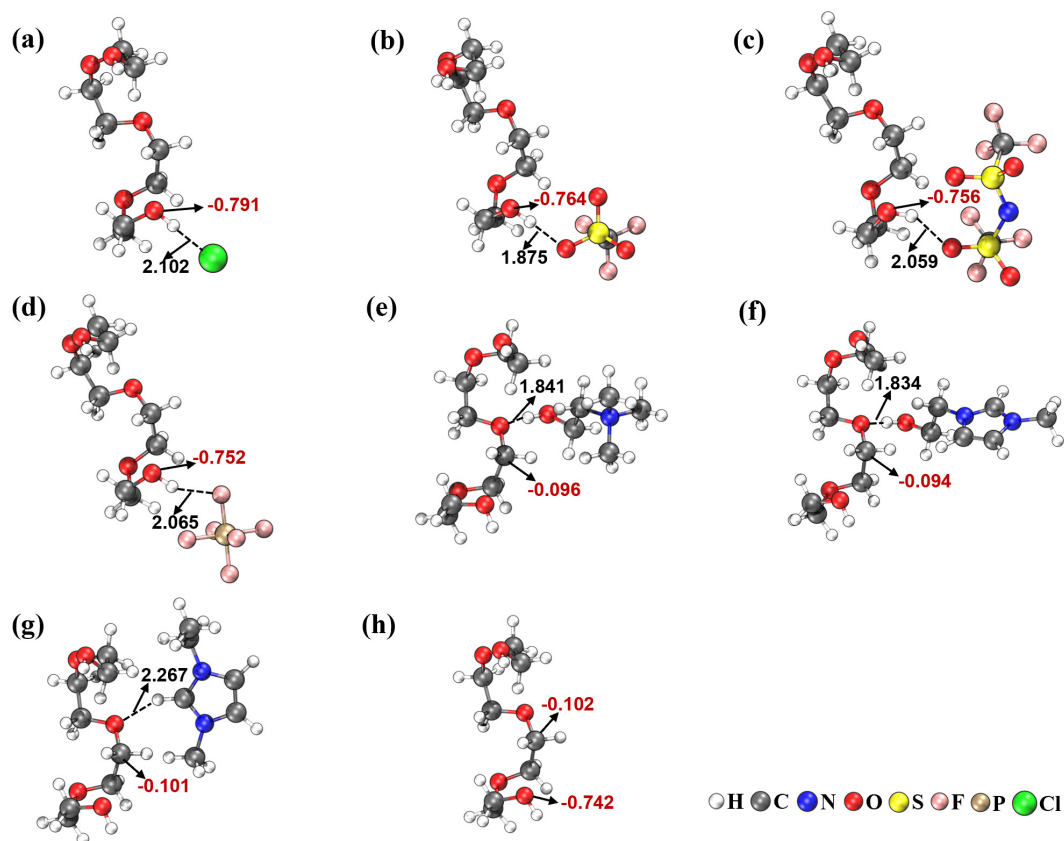
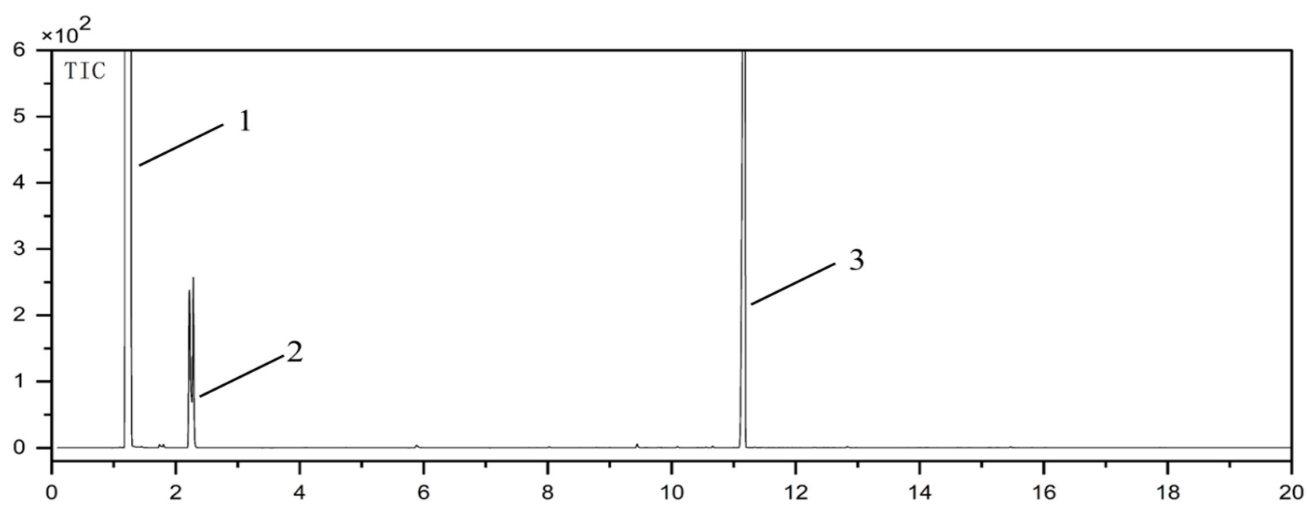
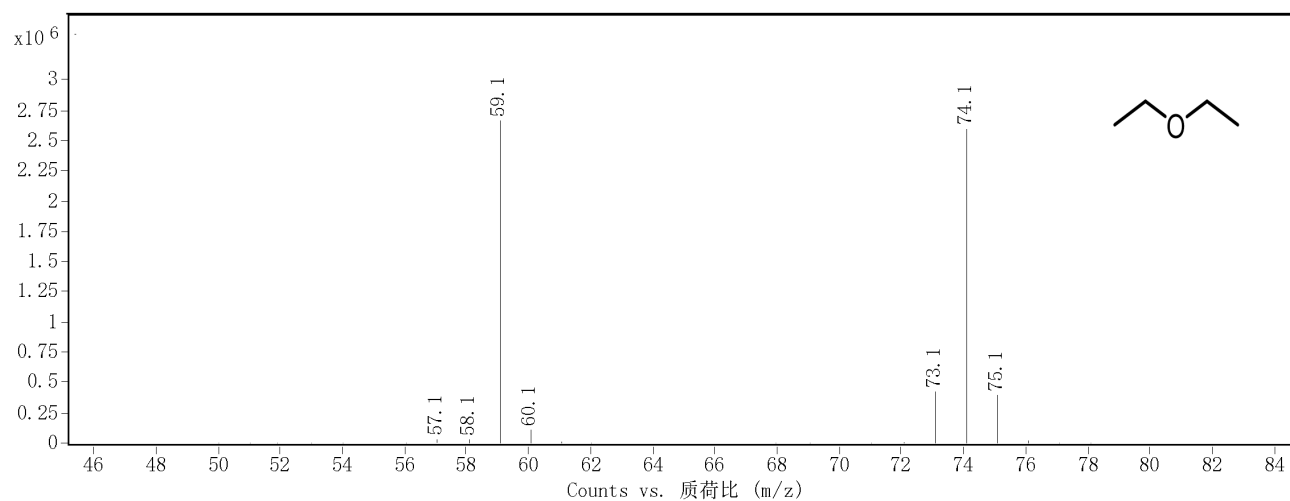
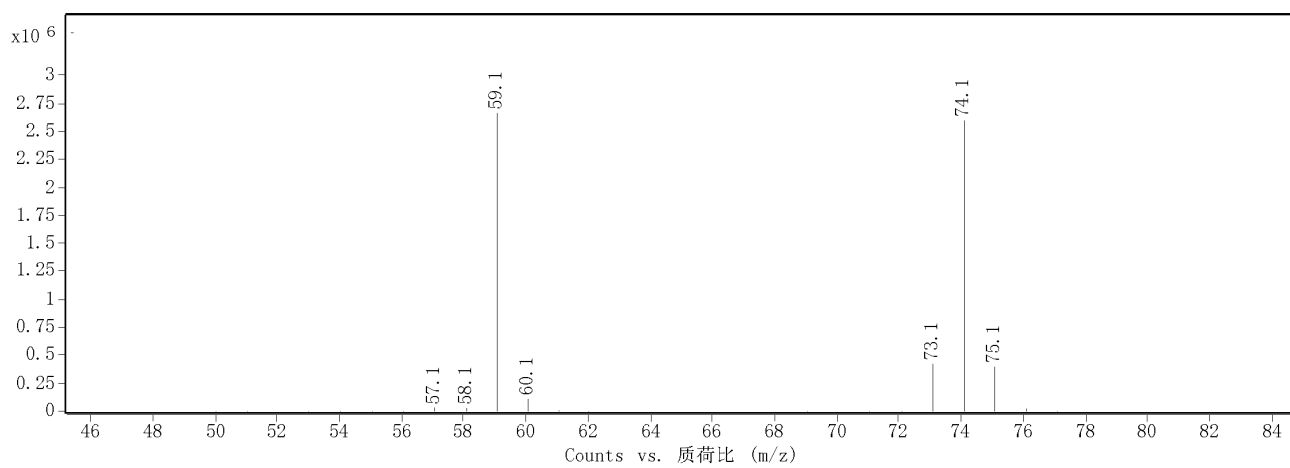


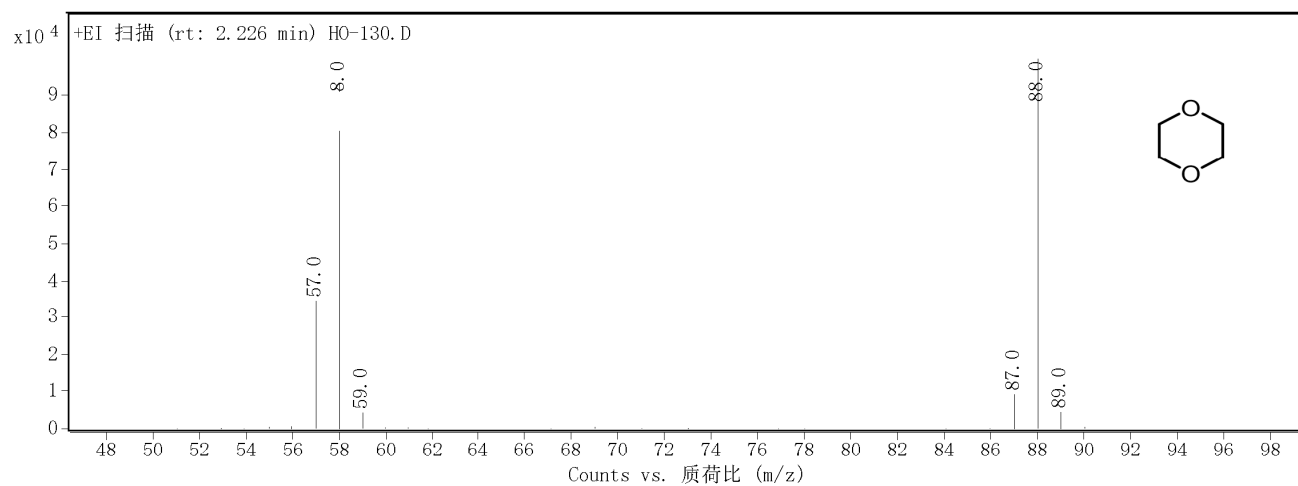
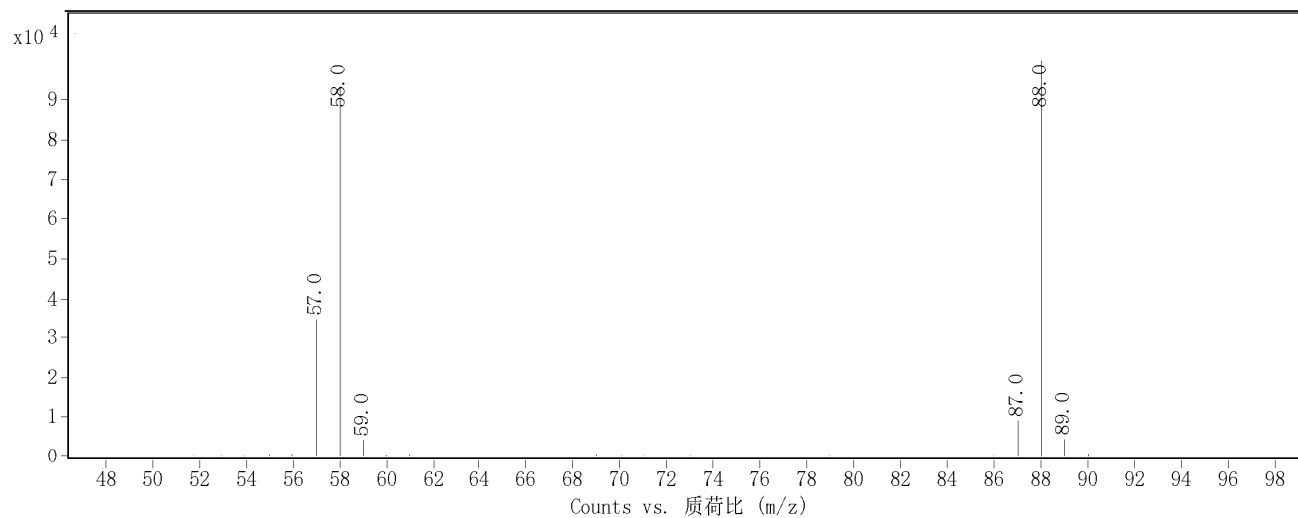
Fig. S2 Possible structures of **M** interacted with (a) Cl^- , (b) $[\text{OTf}]^-$, (c) $[\text{NTf}_2]^-$, (d) $[\text{PF}_6]^-$, (e) $[\text{HO-EtMim}]^+$, (f) $[\text{HO-EtN}_{111}]^+$, (g) $[\text{EtMim}]^+$ and (h) pure **M** optimized at M062X-D3/def2-TZVP level, on which the natural bond orbital (NBO) charges and hydrogen bond distances [red word: NBO charges, black word: atom distance (\AA)] are marked.



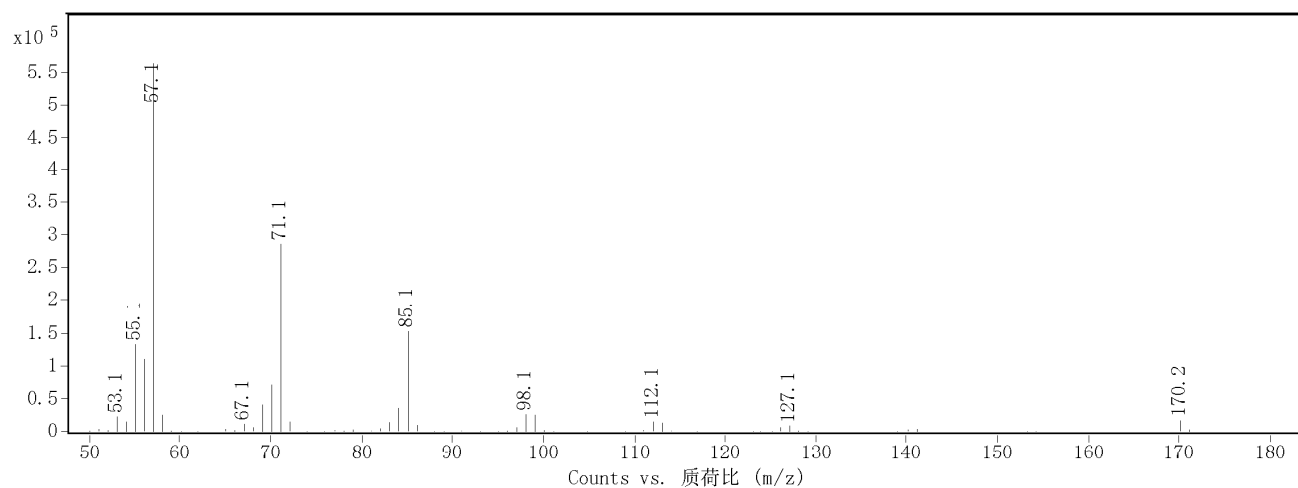
Peak 1



Peak 2



Peak 3



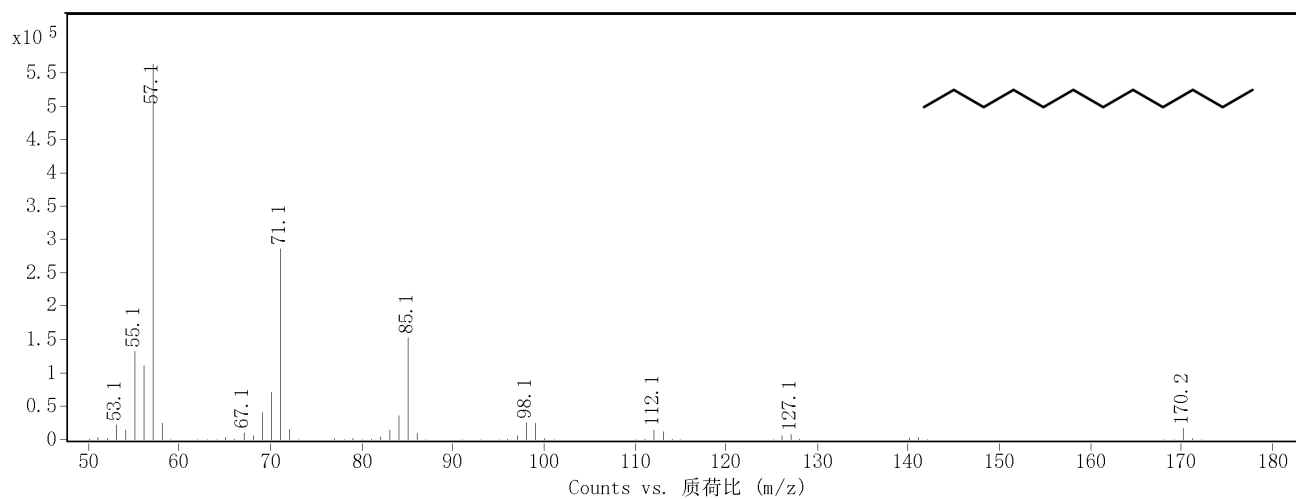


Fig. S3 GC-MS spectra of the product phase after reaction. Reaction conditions: PEG (average Mn: 400, 40 mg), [HO-EtMIm][OTf] (0.4 mmol), 130 °C, 12 h. (Note: Diethyl ether and n-dodecane were the solvent and internal standard, respectively.)

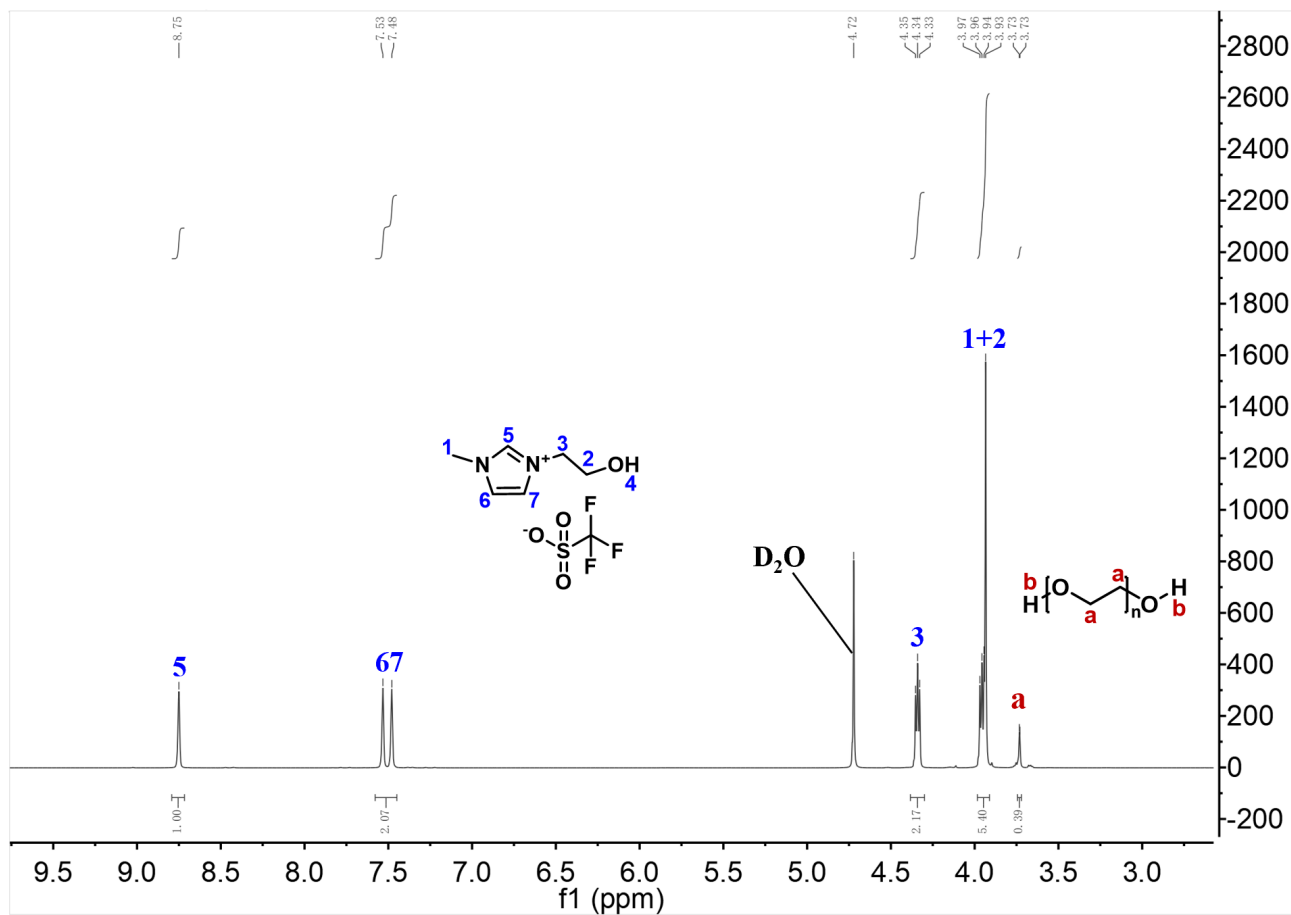


Fig. S4 ^1H NMR spectrum of the IL phase after reaction. Reaction conditions: PEG (average Mn: 400, 40 mg), [HO-EtMim][OTf] (0.4 mmol), 130 °C, 12 h.

Note: From ^1H NMR spectrum of the IL phase, it was clear that only [HO-EtMim][OTf] and very little amount of unreacted PEG were detected, and no 1,4-dioxane were present in the IL phase (Fig. S4). This means that there was no 1,4-dioxane residue in the IL, and IL is stable for the reaction.

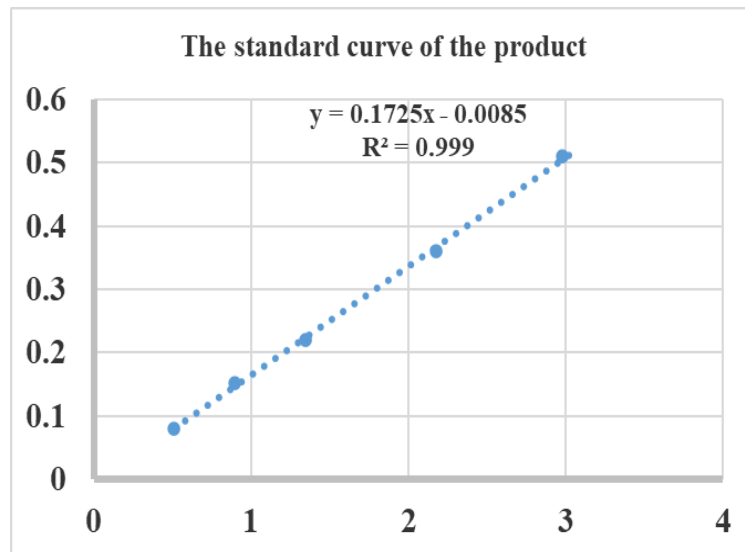


Fig. S5 The standard curve of the product.

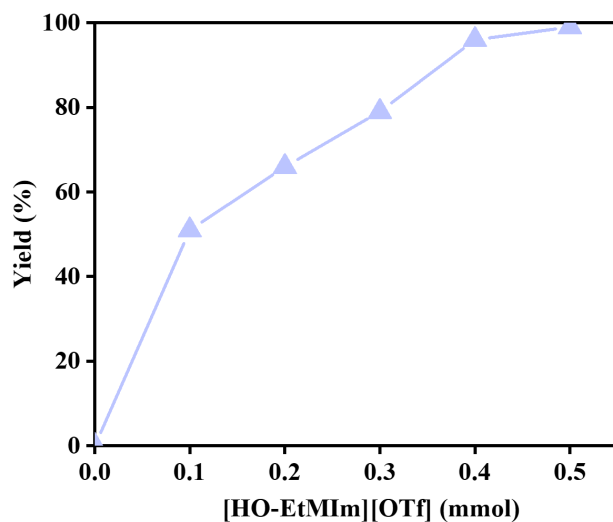
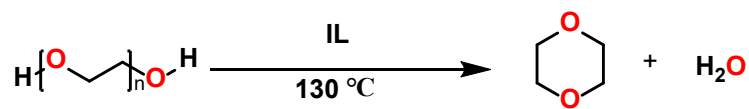


Fig. S6 Effect of the catalyst loadings. Reaction conditions: PEG (average Mn: 400, 40 mg), 12 h, $130\text{ }^\circ\text{C}$. The product yields were determined by GC analysis with n-dodecane as an internal standard.

Note: As shown in Fig. S6, the yield of 1,4-dioxane increased with addition of [HO-EtMIm][OTf] and achieved 99% with 0.5 mmol of [HO-EtMIm][OTf].

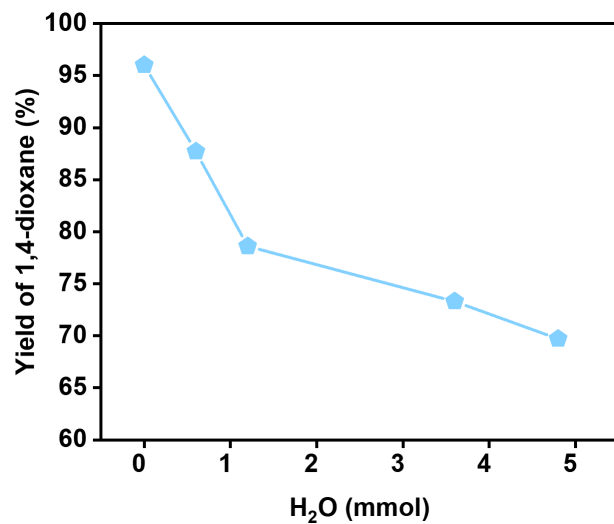


Fig. S7 Effect of water amounts on the degradation of PEG. Reaction conditions: PEG (average Mn: 400, 40 mg), [HO-EtMIm][OTf] (0.4 mmol), 130 °C, 12 h.

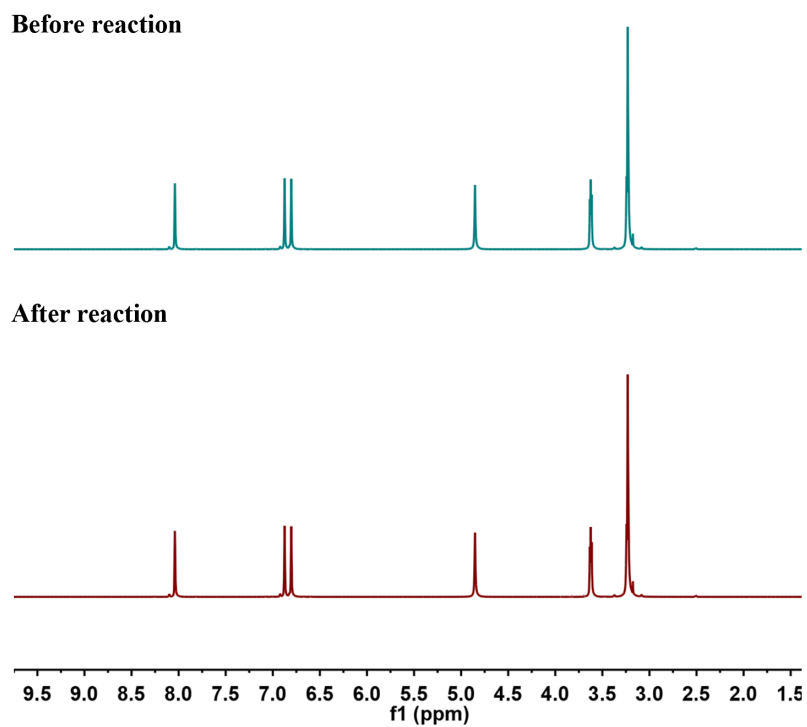


Fig. S8 ¹H NMR spectra of [HO-EtMIm][OTf] before and after reaction.

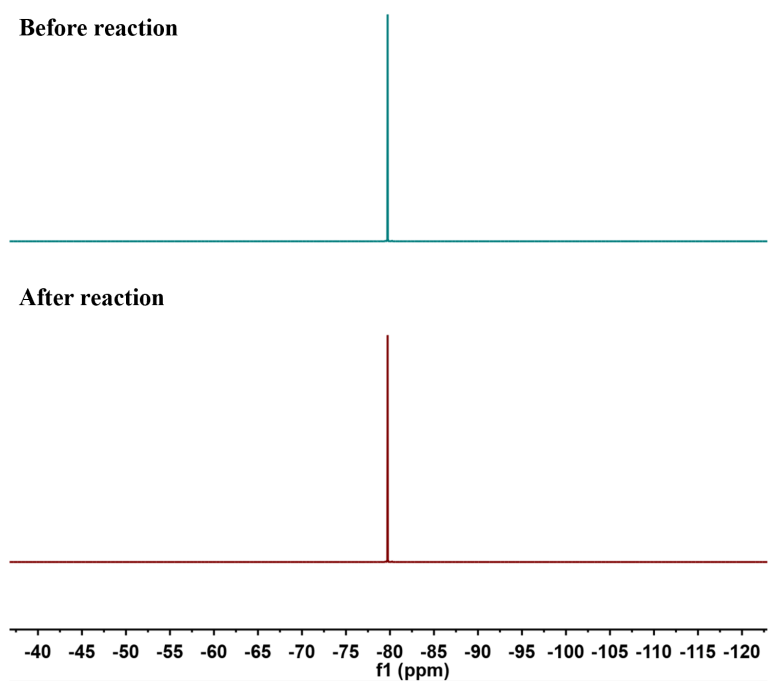


Fig. S9 ^{19}F NMR spectra of [HO-EtMIm][OTf] before and after reaction.

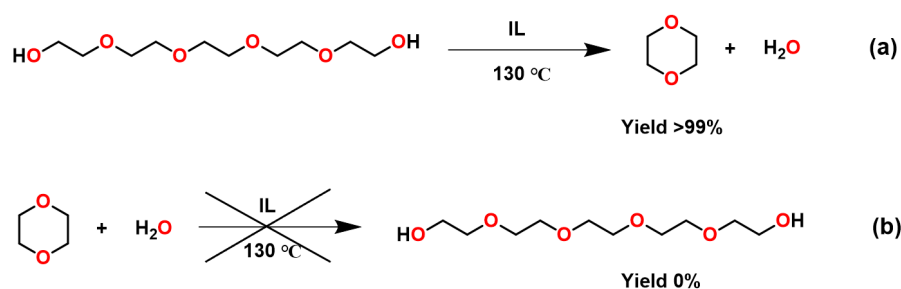


Fig. S10 Control experiment. Reaction conditions: [HOEtMIm][OTf] (0.4 mmol), 130 °C, 12 h for (a) tetraethylene glycol (**M**, 0.3 mmol), and (b) 1,4-dioxane (0.3 mmol), H₂O (0.15 mmol).

Note: As displayed in Fig. S10, the yield of 1,4-dioxane achieved >99% in the reaction **a**, while no **M** was detected in the reaction of 1,4-dioxane and H₂O, indicating that the degradation of PEG to 1,4-dioxane is irreversibly.

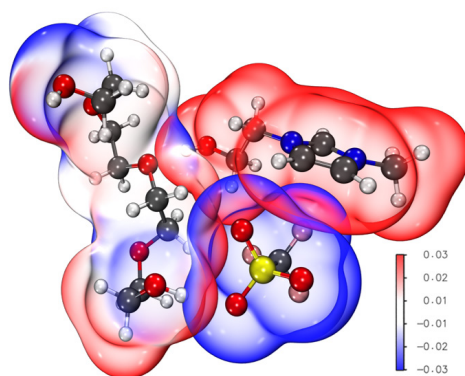


Fig. S11 Electrostatic potential (ESP) distribution of [HO-EtMim][OTf] with **M**.

Note: As shown in Fig. S11, the electrostatic potential (ESP) distribution of **M** with [HO-EtMim][OTf] was performed. Obviously, at the areas where the hydrogen bonds (HBs) formed, the positive surface potentials (red areas) of -OH in **M** and [HO-EtMim]⁺ overlap with the negative surface potentials (blue areas) of O in [OTf]⁻ and ether O in **M**, respectively; indicating the electrostatic attraction of HBs formed between [HO-EtMim][OTf] and **M**.⁶⁻⁸

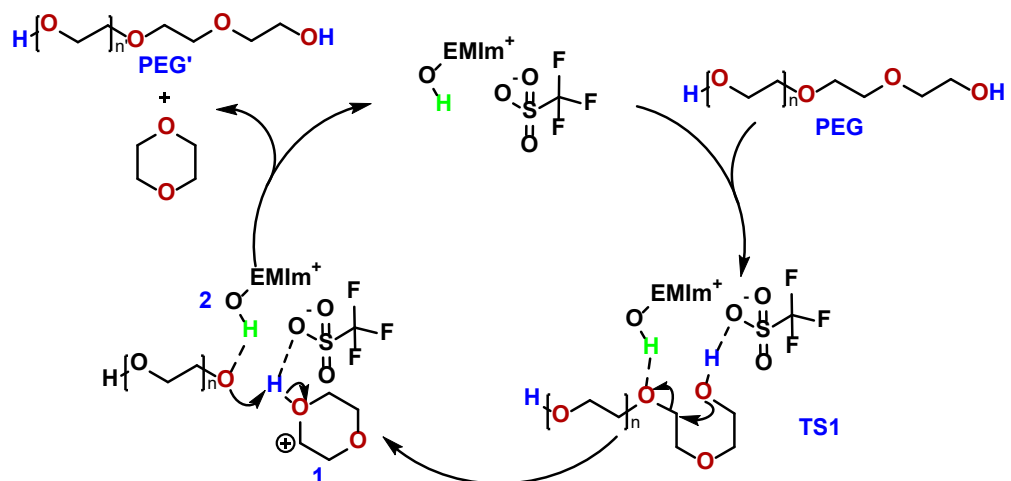


Fig. S12 Proposed reaction pathway.

Table S1 Comparison of various catalysts for the degradation of PEG⁹⁻¹⁵.

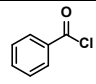
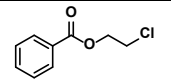
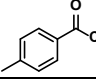
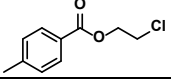
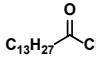
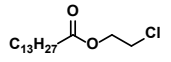
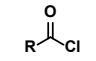
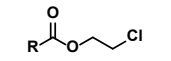
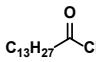
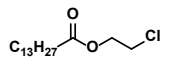
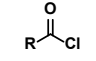
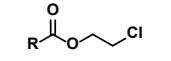
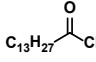
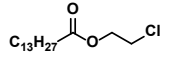
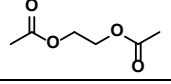
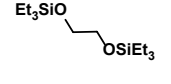
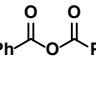
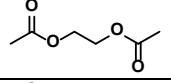
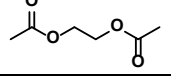
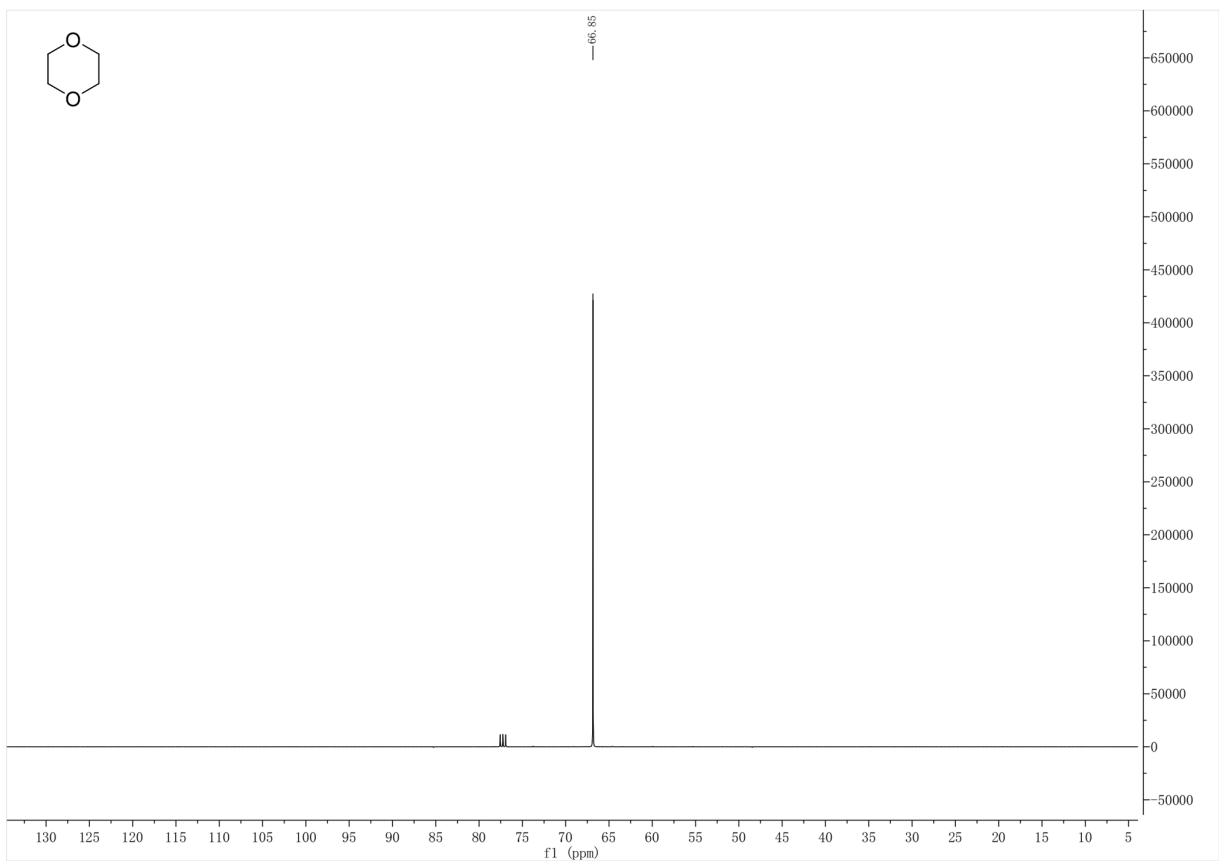
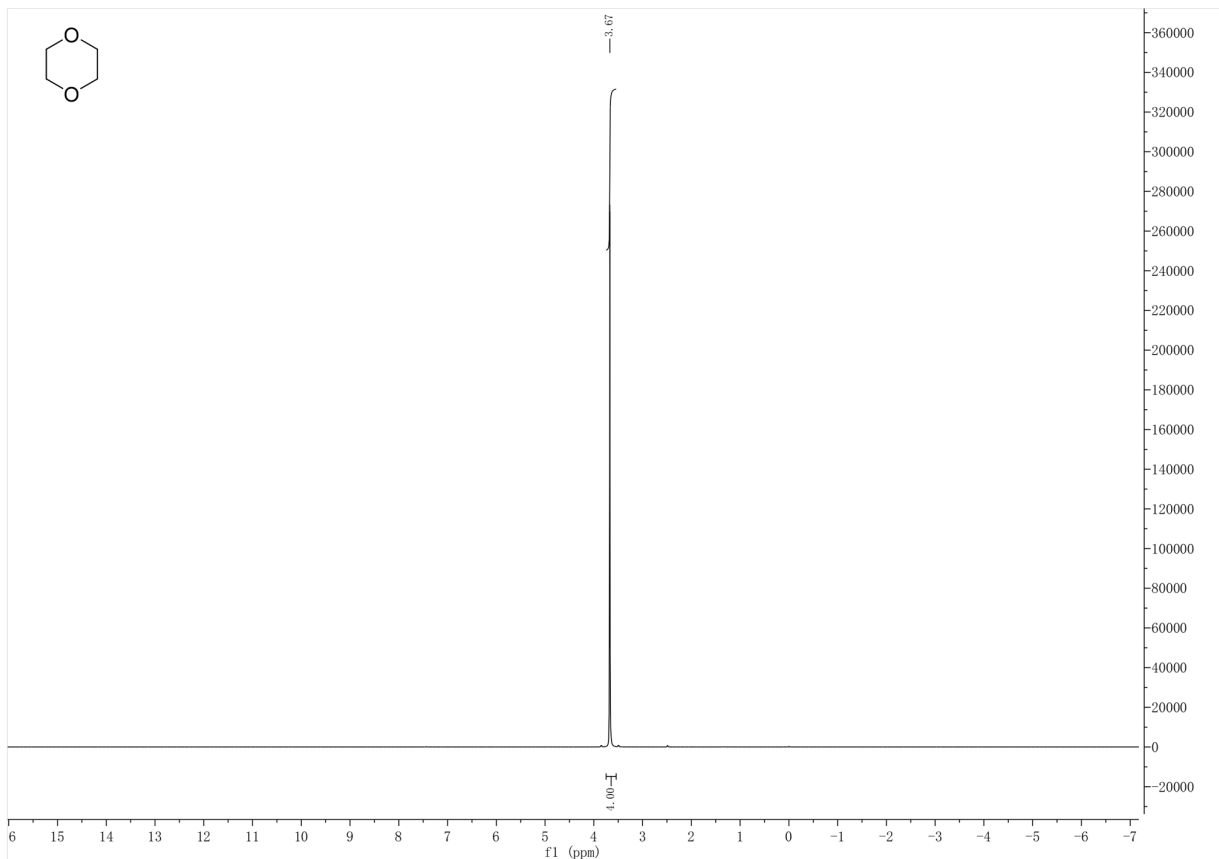
Catalyst	Substrate 1	Substrate 2	Reaction conditions	Product	Yield/%	Ref.
ammonium polyphosphate	PEG Mn ≈ 1000 & 1500	/	200-400 °C	1,4-dioxane	/	[9]
FeCl ₂ ·4H ₂ O	PEG Mn ≈ 100000		100 °C, 24 h		89	[10]
					91	
FeCl ₂ ·4H ₂ O	PEG Mn ≈ 300		100 °C, 24 h		78	[10]
FeCl ₂ ·4H ₂ O	PEG Mn ≈ 300		100 °C, 24 h		75-78	[11]
					69	
ZnCl ₂	PEG Mn ≈ 300		130 °C, 24 h		91-94	[12]
					91	
Zn(OTf) ₂	PEG Mn ≈ 300	Ac ₂ O	150 °C, 24 h		19	[12]
B(C ₆ F ₅) ₃	PEG	Et ₃ SiH	RT, 3h		41	[13]
				C ₂ H ₆	58	
H-mont	PEG Mn ≈ 350		100 °C, 12 h	Glycol dibenzoate	99	[14]
			100 °C, 24 h		86	
H-mont	PEG Mn ≈ 350	Ac ₂ O/AcOH	160 °C, 48 h		92	[14]
H ⁺ -mont	PEG Mn ≈ 400	AcOH	160 °C, 24 h		85	[15]

Table S2 The Kamlet-Taft parameters (α , β) of four typical ionic liquids¹⁶.

IL	Yield of 1,4-dioxane	α	β	α - β
[HO-EtMIm][OTf]	96%	0.797066005	0.875947287	-0.078881281
[HO-EtN ₁₁₁][OTf]	19%	1.121082285	0.411879099	0.709203186
[HO-EtMIm][Cl]	0%	0.797066005	0.84000972	-0.042943715
[HO-EtMIm][ClO ₄]	0%	0.805913554	0.798476096	0.007437458

Note: To investigate the correlation between the catalytic activity of the ionic liquids and their Kamlet-Taft parameters (α , β), the Kamlet-Taft parameters (α , β) of four typical ionic liquids featuring good hydrogen bond donor and acceptor (including [HO-EtMIm][OTf], [HO-EtMIm][Cl], [HO-EtMIm][ClO₄] and [HO-EtN₁₁₁][OTf]) were evaluated (Table S2). The results indicated that there is no correlation between the catalytic activity of the ionic liquids and their Kamlet-Taft parameters (α , β).

NMR spectra:



References

1. M. Frisch, G. W. Trucks, H. B. Schlegel, G. E. Scuseria, M. A. Robb, J. R. Cheeseman, G. Scalmani, V. Barone, B. Mennucci and G. Petersson, *Gaussian, Inc., Wallingford CT*, 2009.
2. Y. Zhao and D. G. Truhlar, *Theor. Chem. Acc.*, 2008, **120**, 215-241.
3. F. Weigend and R. Ahlrichs, *Phys. Chem. Chem. Phys.*, 2005, **7**, 3297-3305.
4. A. V. Marenich, C. J. Cramer and D. G. Truhlar, *J. Phys. Chem. B*, 2009, **113**, 6378-6396.
5. V. S. Bernales, A. V. Marenich, R. Contreras, C. J. Cramer and D. G. Truhlar, *J. Phys. Chem. B*, 2012, **116**, 9122-9129.
6. T. Lu, F. Chen, *J. Comput. Chem.*, 2012, **33**, 580-592.
7. J. Zhang, *J. Chem. Theory Comput.*, 2018, **14**, 572-587.
8. S. Wu, W. Zhang, L. Qi, Y. Ren, H. Ma, *J. Mol. Struct.*, 2019, **1197**, 171-182.
9. N. Grassie and G. A. P. Mendoza, *Polym. Degrad. Stabi.*, 1985, **10**, 43-54.
10. S. Enthaler and M. Weidauer, *ChemSusChem*, 2012, **5**, 1195.
11. S. Enthaler, *Eur. J. Lipid Sci. Technol.*, 2013, **115**, 239-245.
12. S. Enthaler, *Catal. Lett.*, 2014, **144**, 850-859.
13. E. Feghali and T. Cantat, *ChemSusChem*, 2015, **8**, 980-984.
14. Z. Maeno, S. Yamada, T. Mitsudome, T. Mizugaki and K. Jitsukawa, *Green Chem.*, 2017, **19**, 2612-2619.
15. Z. Maeno, K. Midogochi, T. Mitsudome, T. Mizugaki and K. Jitsukawa, *Tetrahedron Lett.*, 2018, **59**, 832-835.
16. Q. Liu, X. Zhao, D. Yu, H. Yu, Y. Zhang, Z. Xue and T. Mu, *Green Chem.*, 2019, **21**, 5291-5297.